



Supporting Information

© Wiley-VCH 2006

69451 Weinheim, Germany

# Designed CO<sub>2</sub>-philes Stabilize Water-in-Carbon Dioxide Microemulsions

Julian Eastoe\*<sup>Ⓢ</sup>, Sarah Gold<sup>Ⓢ</sup>, Sarah Rogers<sup>Ⓢ</sup>, Paul Wyatt<sup>Ⓢ</sup>, David C Steytler<sup>Ⓢ</sup>, Alexandre Gurgel<sup>Ⓢ</sup>, Richard K. Heenan<sup>Ⓢ</sup>, Xin Fan<sup>Ⓢ</sup>, Eric J. Beckman<sup>Ⓢ</sup>, Robert M. Enick<sup>Ⓢ</sup>

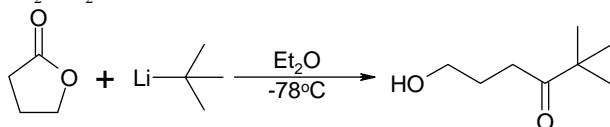
<sup>Ⓢ</sup>School of Chemistry, University of Bristol, Bristol, BS8 1TS, United Kingdom, <sup>Ⓢ</sup>School of Chemical Sciences and Pharmacy, University of East Anglia, Norwich NR4 7TJ, United Kingdom, <sup>Ⓢ</sup>SIS-CCLRC Rutherford Appleton Laboratories, Chilton, OX11 0QX, United Kingdom, and <sup>Ⓢ</sup>Department of Chemical and Petroleum Engineering, University of Pittsburgh, Pittsburgh, PA 15261.

## 1. Synthesis and characterization of AOK and AO-VAc surfactants

### Synthesis of 5,5-dimethyl-hexan-1-ol (1)

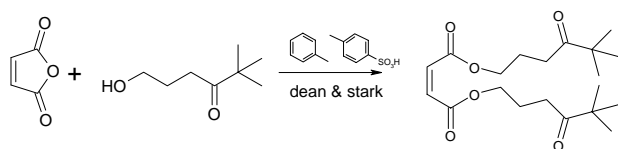
$\gamma$ -Butyrolactone (5.22ml, 68mmol) was dissolved in dry diethyl ether in an inert environment and cooled to  $-78^{\circ}\text{C}$  with stirring. To this mixture, *t*-butyl lithium (44 ml, 1.7 M in pentane, 75 mmol) was added drop wise. After addition was complete the reaction was left at  $-78^{\circ}\text{C}$  for 2 hours before quenching with sat.  $\text{NH}_4\text{Cl}$  (aq) (25 ml) and allowing to warm to room temperature. The mixture was extracted with diethyl ether and washed with 10%  $\text{NaOH}$  (aq) (x 2) and brine. The organic phase was dried over  $\text{MgSO}_4$  and solvent removed to give a colorless oil and white crystalline solid.

The alcohol was purified via distillation ( $105^{\circ}\text{C}$  1mm Hg) to give a colorless oil.  $^1\text{H NMR}$  ( $\text{CDCl}_3$ ): ( $\delta=1.05$ )  $\text{C}(\text{CH}_3)_3$ , ( $\delta=3.63$ )  $\text{C}(\text{O})-\text{CH}_2$ , ( $\delta=2.64$ )  $\text{C}(\text{OH})-\text{CH}_2$ , ( $\delta=1.85$ )  $\text{CH}_2-\text{CH}_2-$



### Synthesis of but-2-enedioic acid bis(5,5-dimethyl-4-oxo-hexyl ester) (2)

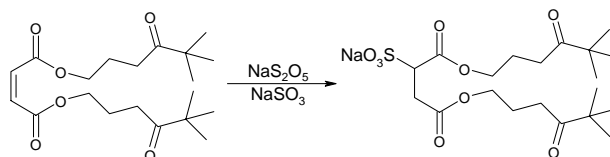
Maleic anhydride (5g, 51 mmol) and 5,5-dimethyl-hexan-1-ol (1) (19.9 g, 153 mmol) was dissolved in toluene (200ml) and *p*-toluene sulfonic acid (0.99 g, 5.75 mmol) added. The reaction mixture was heated to  $110^{\circ}\text{C}$  for 12h and water generated removed via Dean and Stark apparatus. The reaction mixture was washed repeatedly with saturated  $\text{NaHCO}_3$  (aq) solution, the organic phase dried over  $\text{MgSO}_4$  and solvent removed to give an off-white oil.  $^1\text{H NMR}$  ( $\text{CDCl}_3$ ): ( $\delta=1.15$ )  $\text{C}(\text{CH}_3)_3$ , ( $\delta=4.2$ )  $\text{CO}_2\text{CH}_2$ , ( $\delta=1.95$ )  $\text{CH}_2-\text{CH}_2-\text{CH}_2$ , ( $\delta=2.58$ )  $\text{CH}_2-\text{C}(\text{O})-$ , ( $\delta=6.85$ )  $\text{C}=\text{CH}-$



### Synthesis of sodium bis(5,5-dimethyl-4-oxo-hexyloxycarbonyl) sulfosuccinate (AOK)

Di-ester (2) (7.92 g, 21.5 mmol), was dissolved in ethanol (100ml) and water added to saturation.  $\text{Na}_2\text{S}_2\text{O}_5$  (2.2 eq., 9.37 g, 49.3 mmol),  $\text{Na}_2\text{SO}_3$  (1.8 eq., 5g, 40.3 mmol) was then added and the mixture was heated under reflux for 6 h. Solvent was completely removed to give a white solid product, which underwent crude purification via sohxlet extraction using dry distilled  $\text{AcOEt}$ . Further purification was achieved by dissolving in the minimum amount of dry distilled acetone and centrifuging at 6000 rpm for 30 min.

$^1\text{H NMR}$  ( $\text{CDCl}_3$ ): ( $\delta=1.12$ )  $\text{C}(\text{CH}_3)_3$ , ( $\delta=4.15$  &  $4.05$ )  $\text{CO}_2\text{CH}_2$ , ( $\delta=1.87$ )  $\text{CH}_2-\text{CH}_2-\text{CH}$ , ( $\delta=2.98$  &  $3.15$ )  $\text{CH}_2-\text{C}(\text{O})-$ , ( $\delta=2.73$ )  $\text{CH}_2\text{CO}_2$ , ( $\delta=2.65$ )  $\text{CHCO}_2$

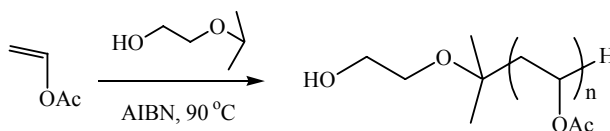


### Dilute aqueous solution behavior of AOK

The surfactant AOK is very water soluble, and dilute aqueous solutions generated stable foams on shaking. The critical micelle concentration (cmc) was determined by electrical conductivity at  $25.0^{\circ}\text{C}$  (Jenway Electrochemistry Analyser). Surfactant solutions were allowed to reach thermal equilibrium in a water bath at  $25.0 \pm 0.5^{\circ}\text{C}$ , before introducing the conductivity probe. The value for AOK ( $10 \pm 2 \text{ mmol dm}^{-3}$ ) compares favorably with normal Aerosol-OT (cmc  $2.6 \text{ mmol dm}^{-3}$  [1]). For AOK the cmc is expected to be slightly higher than for AOT owing to the presence of hydrophilic carbonyl groups in the AOK chains.

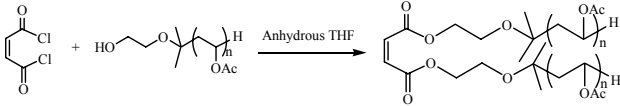
### Synthesis of hydroxy-functional (vinyl acetate)<sub>8</sub> (3)

The 2,2'-azobisisobutyronitrile (AIBN) was recrystallized in methanol, and vinyl acetate was passed over an inhibitor remover column prior to use. Oligomerization of vinyl acetate was carried out using AIBN as a free radical initiator with 2-isopropoxyethanol being both the solvent and chain-transfer agent. A solution of AIBN (0.356 g, 2.17 mmol) in 2-isopropoxyethanol (20 ml) (previously degassed for 30 min) was added to a solution of vinyl acetate (20 ml, 217 mmol) in 2-isopropoxyethanol (360 ml) (previously degassed in a three-neck 500 ml round-bottom flask by bubbling through nitrogen for 30 min). The reaction mixture was refluxed at  $90^{\circ}\text{C}$  under a  $\text{N}_2$  blanket for 24 h. The solvent was removed by rotary evaporation followed by vacuum desiccation at  $90^{\circ}\text{C}$  overnight. A viscous yellow liquid of hydroxy-functional oligo(vinyl acetate) with 8 repeat units, designated PVAc8-OH, was recovered (12 g, yield 64.24%).  $^1\text{H NMR}$  ( $\text{CDCl}_3$ ): ( $\delta=4.89$ )  $\text{CH}_2-\text{CH}$ , ( $\delta=4.08$ )  $\text{OH}-\text{CH}_2-\text{CH}_2$ , ( $\delta=3.59$ )  $\text{OH}-\text{CH}_2-\text{CH}_2$ , ( $\delta=3.43$ )  $\text{OH}$ , ( $\delta=2.03$ )  $\text{C}(\text{CH}_3)_2$ , ( $\delta=1.84$ )  $\text{CH}_2-\text{CH}$ , ( $\delta=1.20$ )  $\text{C}(\text{O})-\text{CH}_3$ .  $^1\text{H NMR}$  spectra showed  $\text{DP}_n = 8$  and  $\text{M}_n = 792 \text{ g mol}^{-1}$ .



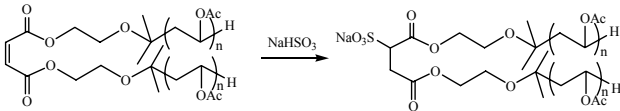
### Synthesis of bis(vinyl acetate)8 ester (4)

Hydroxy-functional (vinyl acetate)8 (3) (10 g, 12.63 mmol) and anhydrous THF (120 ml) were charged in a 250 ml three-neck round-bottom flask equipped with a stirring bar and condenser under a steady flow of nitrogen. After cooling to 0 °C, fumaryl chloride (1.5 eq., 1.45 g, 9.47 mmol) was added dropwise. The reaction mixture was stirred for the next 24 h at room temperature. After rotary evaporation of THF, the mixture was dissolved in 100 ml of diethyl ether and washed with 50 ml of 1 N HCl, 50 ml of saturated NaHCO<sub>3</sub>, and 50 ml of saturated NaCl solutions sequentially. The ether extract was dried over anhydrous Na<sub>2</sub>SO<sub>4</sub> and filtered, then ether was removed by rotary evaporation. A pale yellow oil of ester product was obtained with 72.31% yield (7.6 g). The FTIR spectra showed the disappearance of the OH peak at 3500 cm<sup>-1</sup> and appearance of carbonyl peak at 1750 cm<sup>-1</sup>. <sup>1</sup>H NMR (CDCl<sub>3</sub>): (δ=6.92) C=CH-, (δ=4.89) CH<sub>2</sub>-CH, (δ=4.08) CO<sub>2</sub>-CH<sub>2</sub>-CH<sub>2</sub>, (δ=3.52) CO<sub>2</sub>-CH<sub>2</sub>-CH<sub>2</sub>, (δ=2.05) C(CH<sub>3</sub>)<sub>2</sub>, (δ=1.78) CH<sub>2</sub>-CH, (δ=1.19) C(=O)-CH<sub>3</sub>.



### Synthesis of sodium bis(vinyl acetate)8 sulfosuccinate (AO-VAc)

Sodium hydrogen sulfite (1.5 eq., 0.66 g, 6.31 mmol) in water (120 ml) was added dropwise to a solution of the ester (4) (7 g, 4.21 mmol) in 2-propanol (160 ml) (both solutions were previously degassed with nitrogen for 30 min). The reaction mixture was then refluxed for the next 24 h. After rotary evaporation of the solvent, the residue was dissolved in chloroform and dried over Na<sub>2</sub>SO<sub>4</sub> followed by removal of the solvent and drying of the resulting paste in a vacuum desiccator overnight. A yellow viscous liquid was obtained (6.8 g, yield 92%). <sup>1</sup>H NMR (CDCl<sub>3</sub>): (δ=4.88) CH<sub>2</sub>-CH, (δ=4.08) CO<sub>2</sub>-CH<sub>2</sub>-CH<sub>2</sub>, (δ=3.85) CHCO<sub>2</sub>, (δ=3.70) CH<sub>2</sub>CO<sub>2</sub>, (δ=3.56) CO<sub>2</sub>-CH<sub>2</sub>-CH<sub>2</sub>, (δ=2.03) C(CH<sub>3</sub>)<sub>2</sub>, (δ=1.77) CH<sub>2</sub>-CH, (δ=1.14) C(=O)-CH<sub>3</sub>.



## 2. High-pressure Small-angle Neutron Scattering (HP-SANS)

Small-angle neutron scattering (SANS) was used to characterize the water-in-CO<sub>2</sub> microemulsion structure. Experiments were conducted on the time-of-flight small-angle diffractometer LOQ at ISIS, Rutherford Appleton Laboratory, Didcot, UK [2, 3], in conjunction with the pressure cell described elsewhere [4]. A 12 mm path length was required to optimize sample transmission. D<sub>2</sub>O was used to provide contrast to size the aqueous water pools of the reversed microemulsion droplets. Neutron counts were accumulated over periods of 60 minutes to provide data of sufficient statistical quality, and 10 minutes were allowed for transmission runs. Standard procedures [e.g. 3] for the normalization of raw neutron counts as a function of wavelength  $\lambda = 2.2$  to 10 Å yielded absolute scattering intensities  $I(Q)$  in cm<sup>-1</sup>, where the momentum transfer,  $Q = (4\pi/\lambda)\sin(\theta/2)$  and  $\theta$  is the scattering angle (<7°). Scattering data were corrected for wavelength-dependent transmission factors, background (empty cell and CO<sub>2</sub>) and hydrocarbon incoherent scattering arising from hydrogen in the surfactant [3]. Intensities were also corrected for path length,  $P$ - $T$  induced changes in sample volumes, allowing for various conditions to be compared [5].

## 3. Spherical core-shell form factor

For polydisperse, homogeneous spherical particles the SANS intensity  $I(Q) / \text{cm}^{-1}$  is given by,

$$I(Q) = N_p [P(Q,R) p(R)] S(Q) + B_{inc} \quad (\text{A1})$$

where  $I(Q)$  is the absolute scattering intensity,  $N_p$  is the particle number density,  $P(Q)$  is the single particle form factor,  $p(R)$  is a normalized distribution function, and  $S(Q)$  is the interparticle structure factor, which accounts for interactions. The level  $B_{inc}$  represents a sample-dependent isotropic incoherent background, which is determined by independently measuring the CO<sub>2</sub> solvent for subtraction from the sample + solvent data.

For core-shell spherical particles the general form factor  $P(Q,r)$  is given by [6]

$$P(Q,r) = \frac{16\pi^2}{9} \left[ (\rho_{shell} - \rho_{sol}) 3r_D^3 \left( \frac{\sin Qr_D - Qr_D \cos Qr_D}{(Qr_D)^3} \right) - 3r_c^3 \left( \frac{\sin Qr_c - Qr_c \cos Qr_c}{(Qr_c)^3} \right) \right]^2 + (\rho_{core} - \rho_{sol})^2 3r_c^3 \left( \frac{\sin Qr_c - Qr_c \cos Qr_c}{(Qr_c)^3} \right)^2 \quad (\text{A2})$$

where  $r_D$  is the droplet radius,  $r_c$  the core radius (this parameter is called  $r$  in the main paper, see Figure 3 and Table 1). In line with the configuration presented in Figure 3 of the main paper, the parameters  $\rho_{sol}$ ,  $\rho_{shell}$ ,  $\rho_{core}$  represent the coherent scattering length densities ( $slD$ ) of the CO<sub>2</sub> medium, surfactant shell, and D<sub>2</sub>O core respectively. The interfacial adsorbed layer thickness  $t$  is given by  $r_D - r_c$ . With dilute core-shell particles (volume fraction < 0.05) Ottewill *et al.* [6] were the first to show that a peak can arise in  $I(Q)$ , originating from the form factor only; note that this  $P(Q)$  peak is distinct from any interparticle interferences that are normally manifest in the structure factor  $S(Q)$ .

The dilute water-in-CO<sub>2</sub> systems studied here are located away from phase boundaries, and there is no evidence for attractive  $S(Q)$  in the scattering (absence of low  $Q$  critical scattering Figure 2 main paper). Since the volume fraction concentrations studied here are low (< 0.05), to a good first approximation, volume exclusion inter-particle interactions (hard-sphere structure factor  $S_{HS}(Q)$ ) may be neglected [6, 7]. To test for this, trial fits to the data in Figure 2 of the main paper were carried out; including appropriate  $S_{HS}(Q)$  functions, gave essentially the same structural parameters for the core-shell droplets as without  $S_{HS}(Q)$ , and so in final analyses the structure factor was omitted.

A polydispersity term is included in Eq. A1. This was a Schultz distribution function, [7] defined by an average radius  $\bar{R}$  (called  $r$  in the main paper) and a root mean square (RMS) deviation  $\sigma$  given by

$$\sigma = \left[ \overline{(R - \bar{R})^2} \right]^{1/2} = (\overline{R^2} - \bar{R}^2)^{1/2} = \bar{R} / (Z + 1)^{1/2} \quad (\text{A3})$$

where  $Z$  is a width parameter. The polydispersity reported in Table 1 of the main paper is  $\sigma/r$ . The SANS data were fitted using the interactive FISH program [8], which is a flexible multi-model package comprising a variety of different form factors  $P(Q)$ , structure factors  $S(Q)$ , and polydispersity functions. After extensive fitting trials, with different scattering laws, the most appropriate model for the data shown in Figure 2 of the main paper was found to be for Schultz polydisperse core-shell spheres (based on Eqs. A1, A2 and A3, but omitting  $S(Q)$ ).

#### 4. The “fingerprint” SANS curve for core-shell droplets

Using the form factor given above simulations were performed to explore the effects of changing: (a) internal core radius  $r$  (Figure S1), (b) surfactant shell thickness  $t$  (Figure S2) and (c) solvent scattering length density  $\rho_{\text{solv}}$  (Figure S3). In these calculations the polydispersity  $\sigma/r$  was fixed at 0.15 and the volume fraction was 0.05.

Figures S1-S3 reveal the sensitivity of the core-shell form factor to changes in all three parameters, which are important for characterizing surfactant-stabilized nanodroplets in CO<sub>2</sub>.

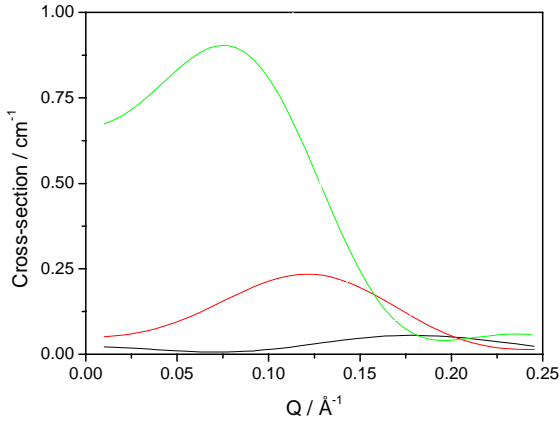


**Figure S1:** Form factor calculations with scattering length densities 2.4, 0.3 and  $6.4 \times 10^{10} \text{ cm}^{-2}$  for the external CO<sub>2</sub> phase, shell and D<sub>2</sub>O core respectively, and a layer thickness  $t = 8 \text{ \AA}$ . The internal D<sub>2</sub>O core radius  $r$  is 15 Å (black), 20 Å (red) and 25 Å (green).

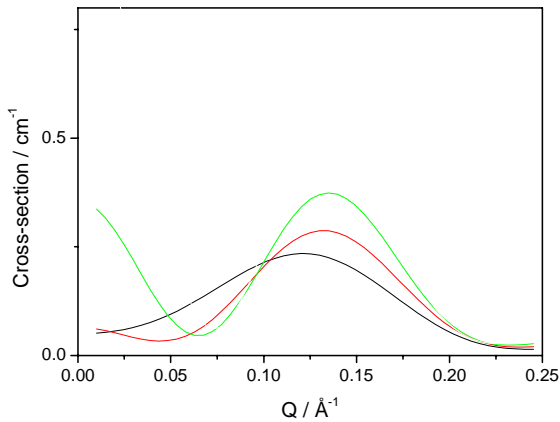


**Figure S2:** Form factor calculations with scattering length densities 2.4, 0.3 and  $6.4 \times 10^{10} \text{ cm}^{-2}$  for the external CO<sub>2</sub> phase, shell and D<sub>2</sub>O core respectively, and an internal D<sub>2</sub>O core radius  $r$  of 20 Å. The layer thickness  $t$  is 8 Å (black), 10 Å (red) and 12 Å (green).

Based on these simulations it can be seen that SANS offers a unique opportunity to experimentally simulate the  $I(Q)$  signal, expected if any given surfactant were to aggregate or microemulsify water in CO<sub>2</sub>. Because the scattering length density  $\rho_{\text{solv}}$  of liquid CO<sub>2</sub> at a typical mass density of  $1 \text{ g cm}^{-3}$  is  $\sim 2.5 \times 10^{10} \text{ cm}^{-2}$  [9], it is possible to formulate a suitable mixture of hydrogen-containing and deuterated hydrocarbon solvents to provide the same value of  $\rho_{\text{solv}}$ . Since most non-ionic surfactants are highly soluble in cyclohexane, this was chosen as a model solvent.

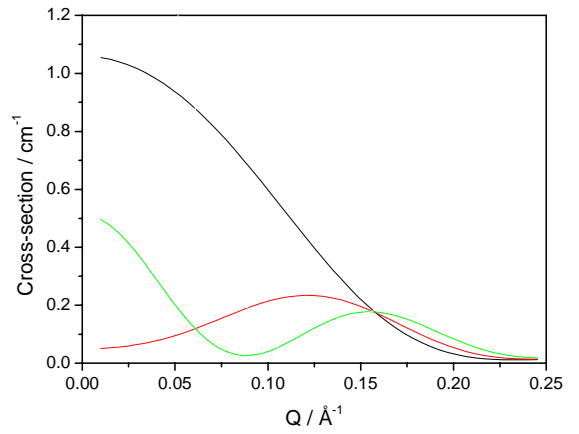


**Figure S3:** Form factor calculations with scattering length densities 0.3 and  $6.4 \times 10^{10} \text{ cm}^{-2}$  for the shell and D<sub>2</sub>O core respectively, an internal D<sub>2</sub>O core radius of  $r = 20 \text{ \AA}$  and an outer layer thickness  $t = 8 \text{ \AA}$ . The scattering length density of the external solvent  $\rho_{\text{solv}}$  is 1.2 (black), 2.4 (red) and 3.6 (green) in units of  $\times 10^{10} \text{ cm}^{-2}$ .

A mixture containing 40% volume of C<sub>6</sub>D<sub>12</sub> (Goss, 99.8% D-atom,  $\rho_{\text{solv}} = +6.7 \times 10^{10} \text{ cm}^{-2}$ ) and 60% volume of C<sub>6</sub>H<sub>12</sub> (Aldrich, 99.9%,  $\rho_{\text{solv}} = -0.28 \times 10^{10} \text{ cm}^{-2}$ ) results in a net solvent scattering length density matched to that of CO<sub>2</sub> i.e.  $2.5 \times 10^{10} \text{ cm}^{-2}$  (of course  $\rho_{\text{CO}_2}$  is pressure and temperature sensitive, but in the liquid region around  $1 \text{ g cm}^{-3}$  there are only small effects [9]). Thus, using this 4:6 D/H cyclohexane mixture as the continuous solvent, and measuring SANS from model water-in-oil (w/o) systems, the scattering profile expected for any given D<sub>2</sub>O core/H-surfactant shell/“CO<sub>2</sub>” microemulsion droplets can be simulated. This type of SANS profile is, therefore, characteristic and can be used as a diagnostic test when compared to the SANS signals observed in real water-in-CO<sub>2</sub> dispersions.

Test SANS experiments were carried out at the D22 diffractometer at ILL (Grenoble, France) using a neutron wavelength of  $\lambda = 10 \text{ \AA}$  at two different detector distances to cover a  $Q$  range of  $0.0024 \rightarrow 0.37 \text{ \AA}^{-1}$ , and also at the time-of-flight LOQ instrument at ISIS, UK where incident wavelengths are  $2.2 \leq \lambda \leq 10 \text{ \AA}$ , resulting in an effective  $Q$  range of  $0.009 \rightarrow 0.249 \text{ \AA}^{-1}$ . Measurements were conducted in 2 mm rectangular quartz cells. The sample compositions were defined by the surfactant concentration in % w/v and the water loading  $w = [\text{D}_2\text{O}]/[\text{surf}]$ .

Figures S4-S6 show the evolution of the SANS profiles, as a function of added D<sub>2</sub>O (increasing  $w$ ) with model non-ionic surfactant Triton X45 (Aldrich) at constant concentration, stabilizing microemulsion droplets in the 4:6 D/H cyclohexane mixture, which simulates liquid CO<sub>2</sub>. It is clear that swelling of the reversed micelles by addition of D<sub>2</sub>O causes dramatic changes: the aggregate dimensions become enlarged, which also introduces a core-shell contrast, resulting in the appearance of a clear peak in the form factor for  $w = 6$  (Figure S6). The data were fitted by the model given in section 3, but modified to give an extra contrast step: radius of the water core ( $r$ ), length of the hydrated EO chain ( $t_{\text{EO}}$ ) and length of the octyl-phenyl hydrophobe ( $t_{\text{tail}}$ ) present in Triton X45. The parameters used, with polydispersity index ( $\sigma/r = 0.20$ ) are given below in Table S1, together with the corresponding  $sld$  values.

$w$	$r$ (Å)	$t_{EO}$ (Å)	$t_{tail}$ (Å)
3	17.5 (6.4)	8.8 (2.5)	8.0 (0.4)
6	23.7 (6.4)	8.8 (2.5)	8.0 (0.4)

**Table S1:** Parameters used to fit low- $w$  microemulsions formed by Triton X45 in a 4:6  $C_6D_{12}/C_6H_{12}$  mixture simulating  $CO_2$ . Fitted  $\rho$  values given in brackets  $\times 10^{10} \text{ cm}^{-2}$ .

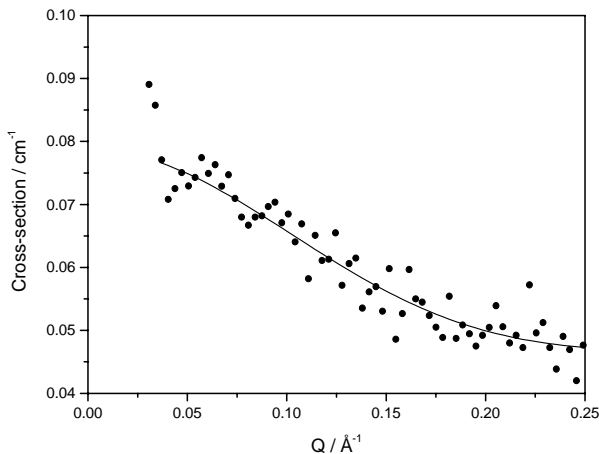


**Figure S4:** SANS data for  $w = 0$  dry reversed micelles of Triton X45 (5% w/v) in a 4:6  $C_6D_{12}/C_6H_{12}$  mixture at 25°C; the symbols are SANS data, and the line is the model fit for a homogenous polydisperse sphere of  $r = 14 \text{ Å}$  and polydispersity 0.20.

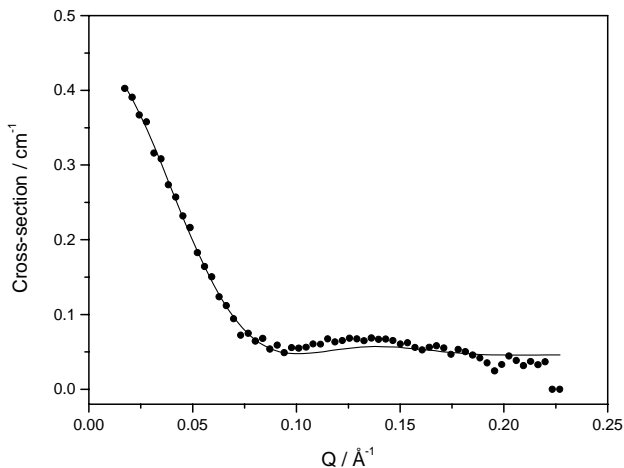


**Figure S5:** SANS data from a Triton X45 (5% w/v) w/o microemulsion with  $w = 3$  in a 4:6  $C_6D_{12}/C_6H_{12}$  mixture at 25°C; the symbols are SANS data and the line is the model fit.

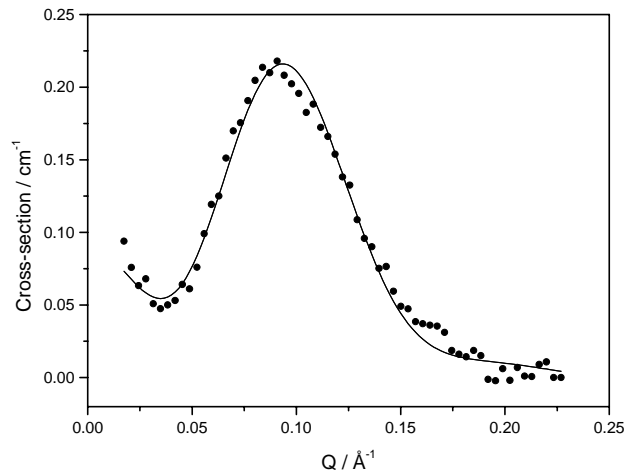


**Figure S6:** SANS data from a Triton X45 (5% w/v) w/o microemulsion with  $w = 6$  in a 4:6  $C_6D_{12}/C_6H_{12}$  mixture at 25°C; the symbols are SANS data and the line is the model fit. The peak originates from the  $P(Q)$  form factor and intraparticle interference effects, rather than an interparticle structure factor  $S(Q)$ , see Figure S1-S3.

Interestingly, Figure S6, shows the clear “fingerprint” form factor peak for SANS from a core-shell structure, with a similar configuration to that given in Figure 3 of the main paper.

## 5. Evaluation of potential and previously claimed stabilizers for w/c systems

HP-SANS experiments were performed on  $D_2O$  and  $CO_2$  systems, with likely candidate surfactants, and also those for which claims of stabilization had previously been made [10, 11]. In these investigations surfactant levels, water concentrations,  $CO_2$  pressure and temperature were all systematically varied (surfactant 1-10 wt%,  $w$  0–20,  $T$  15–50°C,  $P$  50-500 bar). More detail on these experiments can be found elsewhere [12].

### a. Triton non-ionics

Triton X100, Triton X100(reduced) and Triton X45 (all from Aldrich) were all evaluated. Although small changes in the SANS amplitude could be detected on injection of water into Triton nonionics in  $CO_2$  (data not shown), no such responses as given in Figures S1-S3 or S6 were obtained, only very low scattering. The best case scenarios gave weak  $I(Q)$  curves similar to Figure S4, suggesting that true w/c microemulsions cannot be stabilized by these hydrocarbon non-ionic surfactants.

### b. Tergitol® Surfactants

Tergitol® surfactants form a class of nonionic hydrocarbon surfactants possessing a branched 2,6,8-trimethyl-4-nonyl hydrophobe. Stabilization of w/c microemulsions stabilised by Tergitol TMN 6 (Fluka, MW 553, average ethylene oxide number 8.3, HLB 13.1) has been claimed [10]. However the surfactant concentration employed was low such that the  $w$ -values were close to, or even below, the levels of water required to saturate the  $CO_2$  phase itself. The possible formation of w/c microemulsions was therefore tested using the SANS approach outlined above. Before use TMN6 was dried in a desiccator over phosphorous pentoxide for two weeks.

Figures S7 and S8 show test SANS experiments using the 4:6 D/H cyclohexane solvent mixtures. These data were analysed by the core-shell model described above; fitted parameters are given in Table S2 and the functions are shown on the figures. In this case the core region only appears to be comprised of hydrated EO chains.

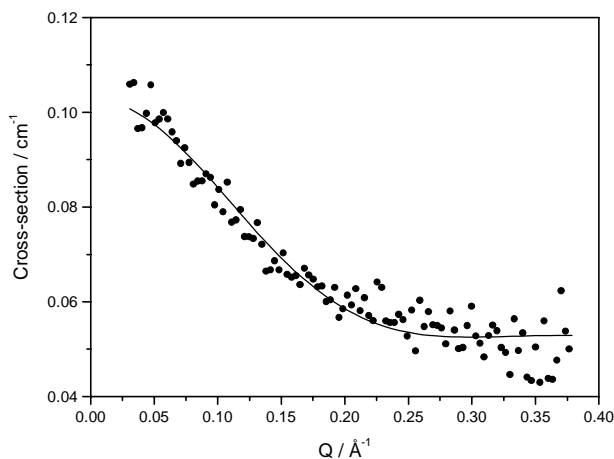


**Figure S7:** SANS data from  $w = 0$  dry reversed micelles of Tergitol TMN 6 (5% w/v) in a 4:6  $C_6D_{12}/C_6H_{12}$  mixture at 25°C; the symbols are SANS data and the line is the model fit.

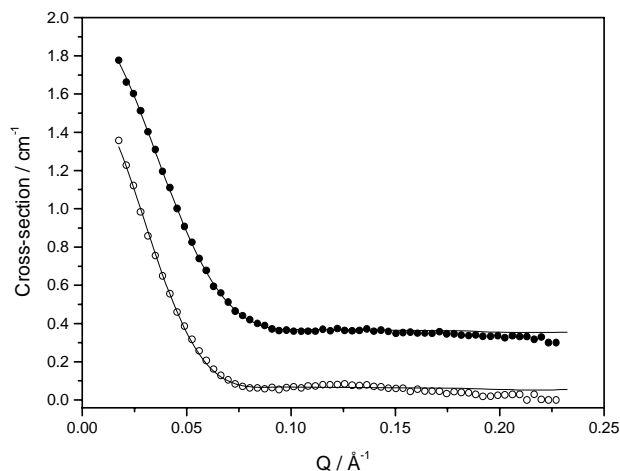


**Figure S8:** SANS data from Tergitol TMN 6 (5% w/v) w/o microemulsions in a 4:6  $C_6D_{12}/C_6H_{12}$  mixture at 25°C; approximate water content: (●)  $w = 3$ ; (○)  $w = 6$ ; the symbols are SANS data and the lines are model fits.

$w$	$r$ (Å)	$t$ (Å)
0	5.5 (0.4)	9 (0.4)
3	28 (1.3)	9 (0.4)
6	34 (1.9)	9 (0.4)

**Table S2:** Parameters used to fit low- $w$  microemulsions formed by Tergitol TMN 6 in a 4:6  $C_6D_{12}/C_6H_{12}$  mixture. Numbers quoted in brackets represent  $\rho$  values in units of  $10^{10} \text{ cm}^{-2}$ .

Next  $D_2O$ -TMN 6- $CO_2$  mixed systems were interrogated by HP-SANS, the measured  $I(Q)$  data and analyses are shown in Figure S9. The response to water injection appears to enhance micelle formation in  $CO_2$ , possibly through H-bonding interactions with low levels of water hydrating the EO chains. However, there was no indication of true w/c microemulsion formation by this surfactant. The data were fitted to a Schulz polydisperse sphere model [7, 8]. With increasing  $w$  value the data give some suggestion of an increase in amplitude and radius (from  $\sim 12.0 \text{ \AA}$  to  $\sim 16.0 \text{ \AA}$ ), but intensities were still low, and the higher  $w$ -values are certainly not typical of microemulsion systems in  $CO_2$ . Importantly, none of the curves in Figure S9 bear any resemblance to the “expected” scattering shown in Figures S1-S3 and S6.

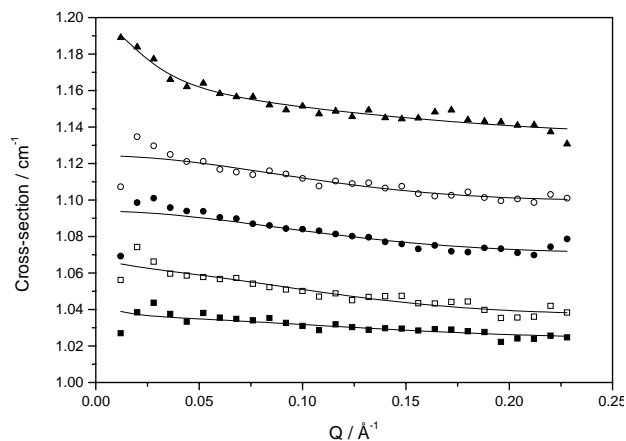


**Figure S9:** SANS data from water- $CO_2$  mixtures in the presence of Tergitol TMN 6 at 50°C and 500 bar; approximate water content: (■)  $w = 0$ ; (□)  $w = 2.9$ ; (●)  $w = 5.8$ ; (○)  $w = 8.7$ ; (▲)  $w = 11.6$ ; the symbols are SANS data and the lines are model fits to a polydisperse sphere model [7, 8]. The curves are shifted vertically for clarity of presentation.

### c. Dynol Surfactants

Dynol surfactants are a series of 2,5,8,11-tetramethyl-6-dodecyn-5,8-diol ethoxylate nonionic amphiphiles possessing a methylated acetylenic structure. It has been claimed that surfactants from this class, like Dynol 604, stabilize water-in- $CO_2$  microemulsions [11]. Figures S10 and S11 show results of HP-SANS experiments with this compound. As was indicated for Tergitol TMN 6, added water appears to induce micelle formation probably by increasing hydrogen bonding in the core. However, the data do not resemble those expected for a true w/c microemulsion of this water content. It was found that Dynol 604 does not stabilise microemulsions in cyclohexane, so the approach adopted previously to simulate scattering from a “ $CO_2$ -like” oil medium could not be applied here.

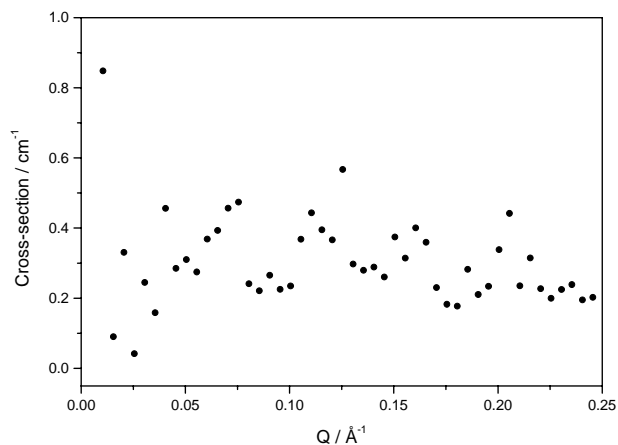


**Figure S10:** SANS data from a Dynol 604 (~5 wt%) solution in carbon dioxide taken at 35°C and 360 bar.

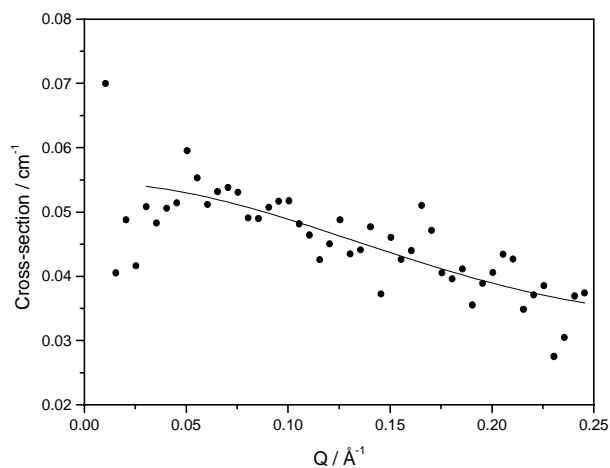


**Figure S11:** SANS data of a Dynol 604 (~ 5 wt%) and D<sub>2</sub>O (~ 1.8 wt%) mixture in carbon dioxide taken at 35°C and 450 bar. Line is fit to a polydisperse sphere model giving a mean radius of ~11.0 Å for the micelles, and polydispersity 0.22.

## References

1. a) S. Nave, J. Eastoe, J. Penfold, *Langmuir* **2000**, 16, 8733; b) S. Nave, J. Eastoe, R.K. Heenan, D.C. Steytler, I. Grillo, *Langmuir* **2000**, 16, 8741.
2. R.K. Heenan, J. Penfold, S. M. King, *J. Appl. Crystallogr.* **1997**, 30, 1140.
3. A.R. Rennie, Reduction of data from SANS instruments. In *Modern aspects of small-angle neutron scattering*; Brumberger edition; NATO ASI Series C; vol. 451; Kluwer Academic Press: USA, 1995, pp 93-105.
4. J. Eastoe, B. H. Robinson, D.C. Steytler, *J.Chem.Soc. Faraday Trans.* **1990**, 86, 511.
5. A. Paul, PhD Thesis University of Bristol, UK. 2001.
6. I. Markovic, R.H. Ottewill, D.J. Cebula, I. Field, J. Marsh, *Col.Polym.Sci.* **1984**, 262, 648.
7. M. Kotlarchyk, S-H. Chen, J.S. Huang, M.W. Kim, *Phys.Rev.A.* **1984**, 29, 2054.
8. R.K. Heenan, *FISH Data Analysis Program*; Rutherford Appleton Laboratory; Report RAL-89-129; CCLRC: Didcot, U.K., **1989**, contact [rkh@isis.rl.ac.uk](mailto:rkh@isis.rl.ac.uk).
9. J.B. McClain, D. Londono, J.R. Combes, T.J. Romack, D.A. Canelas, L. Betts, G.D. Wignall, E.T. Samulski, J.M. DeSimone, *J. Am. Chem. Soc.* **1996**, 118, 917.
10. W. Ryoo, S.E. Webber, K.P. Johnston, *Ind.Eng.Chem.Res.* **2003**, 42, 6348.
11. a) J. Liu, B. Han, J. Zhang, G. Li, X. Zhang, J. Wang, B. Dong, *Chem. Eur. J.* **2002**, 8, 1356; b) J. Liu, B. Han, G. Li, X. Zhang, J. He, Z. Liu, *Langmuir* **2001**, 17, 8040; c) J. Liu, J. Zhang, M. Tiancheng, B. Han, G. Li, J. Wang, B. Dong, *J. Supercrit. Fluid.* **2003**, 26, 27511; d) J. Liu, B. Han, Z. Wang, J. Zhang, G. Li, G Yang, *Langmuir* **2002**, 18, 3086.
12. A. Gurgel, PhD Thesis University of East Anglia, UK. 2004.